# RF Energy Harvester with Constant Off-Time Charger for Batteryless Devices

Mahmoud Gshash, Vishak Narayanan, Henry Duwe and Nathan M. Neihart Department of Electrical and Computer Engineering, Iowa State University, Ames, Iowa, USA {mmgshash, vishakn, duwe, neihart}@iastate.edu

Abstract—Traditional batteryless radio frequency energy harvesting systems are promising for realizing low-cost Internet of Things devices. However, due to variations in the received power, such systems suffer from unpredictable charging time, which can be critical for multi-node communication or in controlling the system's throughput. This paper presents a batteryless RF energy harvester that provides a predictable charging time which is resilient to changes in input RF power, improving system uncertainty. The proposed system is fabricated using commercially available discrete parts to power an MSP430F5594 microcontroller and a CC1352R wireless transceiver. The maximum variation in the measured charging time of the proposed system is only 1.5 seconds as the RF input power is swept from -4 dBm to +9 dBm. The maximum variation in the measured charging time for a traditional energy harvester under the same conditions is 17.3 seconds.

Keywords—batteryless, IoT, RF energy harvester, synchronization, wireless power

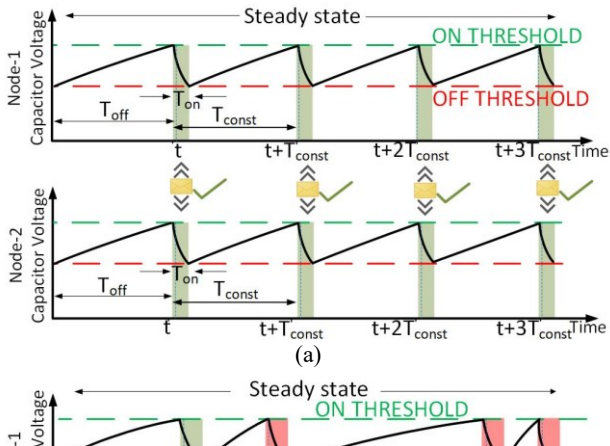
#### I. Introduction

Low-power electronics with small footprints have enabled the creation of IoT devices for various applications, such as infrastructure health, home automation, and monitoring [1]. Most IoT devices require digital control, processing via a microcontroller, and wireless communication, which leads to a relatively high energy requirement [2]. Therefore, most IoT devices rely on a dedicated battery. Given the incredible growth of IoT devices, however, batteries are becoming problematic due to their cost, size, and increased maintenance requirements [3]. To address the problem of battery cost and maintenance, an RF energy harvester can be used to trickle charge the battery [4], but this does not solve the issues of size and weight. The next step to make these systems more economical is to use an external energy source, like a dedicated RF energy transmitter/harvester, and eliminate the battery altogether [5]–[7].

Researchers in recent years have investigated batteryless sensor nodes as an alternative to traditional battery-powered IoT devices [1]–[3]. However, the absence of a battery presents unique challenges, such as limitations in energy density and vulnerability to variations in the energy source [4]. Prior studies have focused on implementing dynamic energy storage options [2]. Nonetheless, relying solely on an RF energy harvester is unlikely to provide sufficient energy for continuous operation. Instead, a batteryless device can intermittently operate by utilizing energy accumulated on a storage element

A primary challenge with this type of intermittent operation occurs when building networks of these devices that must communicate with one another. A simple case can be illustrated by the communication between two intermittently operating

This work was supported in part by the U.S. National Science Foundation under Grant 2008548.



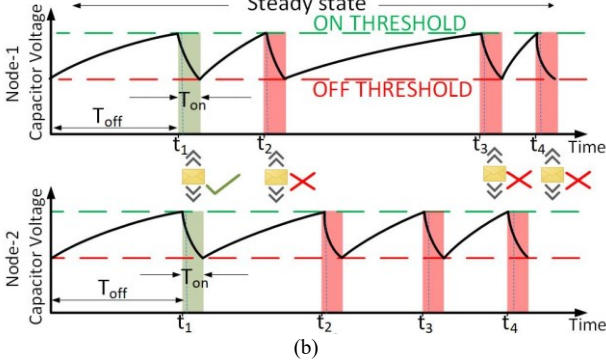


Fig. 1. Two nodes synchronization for (a) uncontrollable off-time, (b) controllable off-time

nodes. As shown in Fig. 1(a), the two nodes must be ON simultaneously for effective communication. The time it takes a single node to fully charge, and turn on, is inversely proportional to the RF power that is incident on the energy harvester. Unfortunately, differences in path loss, shadowing, and other environmental effects, will result in variations in RF power received by the energy harvester [5]. Consequently, without some form of control, the two nodes will eventually lose synchronization, as depicted in Fig. 1(b).

Several methods have been proposed to address synchronization and enhance communication performance in batteryless networks. For example, Deep et al. [9] proposed a synchronization protocol based on rendezvous points, which requires software intervention and is prone to clock errors [6], [7]. Backscatter communication protocols have also gained attention, where devices transmit packets only when sufficient energy is available [8]. In [13] and [14], connection protocols were proposed that rely on a bootstrapping mechanism during initial contact to tackle synchronization issues. While promising, these systems require continuous power to keep the microcontroller in sleep mode, ultimately resulting in a depleted energy due to insufficient replenishing energy.

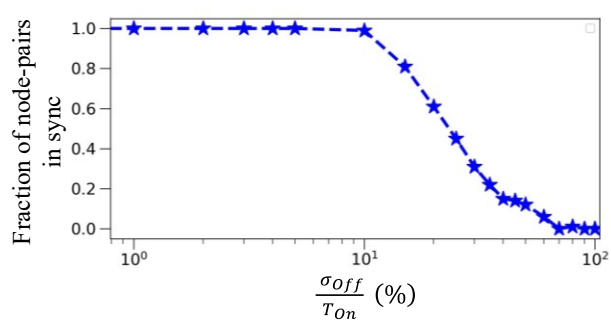


Fig. 2. Fraction of 100 node-pairs that remained synchronized after 10 complete charging cycles versus variation in the off-time, normalize to a constant on-time of 30 msec

Maintaining synchronization in intermittently operating networks remains a fundamental challenge due to variations in RF power incident on the energy harvester, which is directly coupled with the charging time. To address this issue, the proposed system consists of an RF-to-DC converter, a DC regulator, and a constant off-time circuit. The constant off-time circuit makes the charging time robust against input power variations, resulting in more predictable communication and synchronization. The RF-to-DC converter's sensitivity and efficiency have been extensively studied and optimized in the literature [11]–[13]. Moreover, the DC regulator is composed of readily available components that are frequently utilized in energy harvesting applications [14]–[16]. This paper presents a constant off-time circuit, which enables the system to operate with a constant and predictable charging time, independent of variation in input RF power levels given a minimum input threshold. The effectiveness of the proposed system is demonstrated by supplying a node consisting of a microcontroller and wireless transmitter from a wireless power transmitter operating at 915 MHz.

## II. SYNCHRONIZATION IN BATTERYLESS DEVICES

Before we present the proposed constant off-time circuit, we investigate the relationship between the variation in the off-time, referred to as  $T_{off}$ , and the ability of two nodes to remain synchronized in a system-level simulation. This simulation will provide a better understanding of the effect of variations in  $T_{off}$ on synchronization. We assumed that each node has a constant on-time,  $T_{on}$ , and a randomly varying off-time. The variation in the off-time of each node,  $\sigma_{Off}$ , was modeled discretely as a random walk, with each step being a random number sampled from a Gaussian distribution centered on the mean off-time. The variation in the off-time was then normalized by the constant ontime, and we defined two nodes, i and j, as remaining synchronized if the following condition is met:

$$\left|\sigma_{Off(i)} - \sigma_{Off(i)}\right| \le T_{on} \tag{1}$$

 $\left|\sigma_{off(i)} - \sigma_{off(j)}\right| \le T_{\rm on}$  (1) A total of 100 node pairs were simulated with  $T_{on(i)} =$  $T_{on(i)} = 30$  ms, which is the time required for a node to boot and ensure a communication packet [17], and the fraction of node-pairs that remained in synchronization after ten complete charging cycles is shown in Fig. 2. Assuming that all nodes are in sync at the very first charging cycle,  $\sigma_{Off(i)} = \sigma_{Off(j)} = 0$ , It is seen in Fig. 2 that for variations in the off-time of less than 10% of the on-time, approximately 100% of the node-pairs remained synchronized after 10 charging cycles. As the

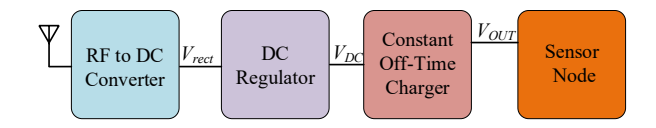
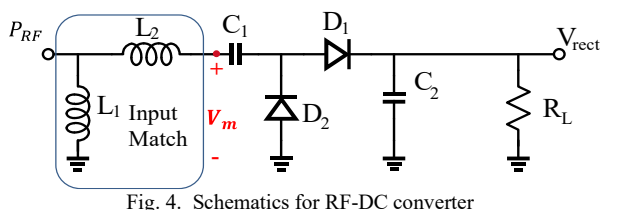


Fig. 3. Block diagram of the proposed energy harvester with constant offtime charger



variation in charging time worsens, however, the number of node-pairs remaining synchronized begins to fall, with 40% variation with respect to the on-time resulting in less than 20% of the node-pairs remaining synchronized.

## III. RF to DC Converter

A transmitter with 3 W EIRP and operating in the 915 MHz ISM-band is used as the dedicated wireless energy source. The AC power received from this transmitter is converted into DC power by the RF to DC converter. The power received by rectifier  $P_{RF}$  can be estimated using Friis transmission equation [18]:

$$P_{RF} = \left(\frac{\lambda}{4\pi D}\right)^2 P_T G_T G_R \tag{2}$$

 $P_{RF} = \left(\frac{\lambda}{4\pi D}\right)^2 P_T G_T G_R \tag{2}$  where  $\lambda$  is the wavelength, D is the separation distance between the transmitter and the receiving antenna, and G is the antenna's gain. The subscripts T and R denote the transmitter and the receiver, respectively. The antenna is connected to a single-stage Dickson multiplier [19] using an RF matching network, Fig 4. The efficiency of the rectifier is a function of the input RF power and the load impedance; therefore, the rectifier was designed for 0 dBm input power and the optimal load was found to be 2.2  $k\Omega$ . At optimal load, the rectifier's DC output is 0.72V, translating to 25% efficiency. Further improvement in efficiency will increase the charging current. However, the efficiency of the rectifier is not a factor in the variation of the charging time.

# IV. CONSTANT OFF-TIME CIRCUIT AND DC REGULATOR A. Constant Off-Time Charger:

The circuit schematic of the constant off-time charger is shown in Fig. 5. Initially, the switch is open, and the load is not connected to the constant off-time circuit. A constant current,  $I_{Cha}$ , is used to charge the primary energy storage capacitor,  $C_{Buf}$ . Assuming that  $I_{Chg}$  is constant, then the voltage drops  $C_{Buf}$ . Assuming that  $C_{CAP}$  is given as:  $V_{CAP}(t) = \frac{I_{Chg}}{C_{Buf}}t$ 

$$V_{CAP}(t) = \frac{r_{Chg}}{c_{Buf}}t\tag{3}$$

A comparator with hysteresis is used to monitor the capacitor voltage, and when  $V_{CAP}$  reaches a predetermined maximum level, the switch is closed, thereby allowing the load to consume the energy stored in the capacitor  $C_{Buf}$ . As the load draws energy from the capacitor,  $V_{CAP}$  is discharged. When  $V_{CAP}$  reaches a predetermined minimum value, the switch is opened, and the load is once again disconnected from the energy source. The voltages for which the switch changes state are expressed by the equations of the hysteretic non-inverting comparator:

$$V_{on} = V_{REF} \left( 1 + \frac{R_3}{R_4} \right) \tag{4}$$

$$V_{on} = V_{REF} \left( 1 + \frac{R_3}{R_4} \right)$$

$$V_{off} = V_{REF} \left( 1 + \frac{R_3}{R_4} \right) - V_{DC} \left( \frac{R_3}{R_4} \right)$$
where  $V_{REF}$  is a reference voltage, expressed as:
$$V_{REF} = V_{DC} \left( \frac{R_2}{R_1 + R_2} \right)$$
(6)

$$V_{REF} = V_{DC} \left( \frac{R_2}{R_1 + R_2} \right) \tag{6}$$

A voltage divider is used to set  $V_{REF}$  to ensure flexibility in choosing  $V_{on}$  and  $V_{off}$ . The above equations assume that the comparator has a rail-to-rail output and that the comparator is powered from  $V_{DC}$ , as shown in Fig. 5.

A constant off-time is achieved by controlling the values of  $V_{on}$  and  $V_{off}$ , and can be expressed using (3) as:

$$T_{off} = \frac{c_{Buf}}{I_{Chg}} (V_{on} - V_{off}) \tag{7}$$
 In addition to achieving a constant off-time, using a constant

current source offers two benefits: 1) It eliminates the dependence of  $T_{Off}$  on RF input power, which is common in conventional wireless energy harvesting systems; and 2) It restricts the current flowing into the energy storage capacitor to a level that the RF-to-DC converter can handle.

## B. DC regulator

The DC regulator circuit sits between the RF-to-DC converter, as shown in Fig. 4, and the constant off-time circuit, shown in Fig. 5. The DC regulator is essential for several reasons. First, the DC regulator is required to efficiently step up the low output voltage of the RF-to-DC converter to power the constant off-time circuit. The supply voltage of the constant offtime circuit must be able to handle the maximum voltage stored on  $V_{CAP}$  in addition to the voltage overhead of the constant current source. A low minimum startup voltage is desirable for improving the system's sensitivity. Second, the DC regulator should also present the optimal load impedance to the RF-to-DC converter for achieving maximum power conversion efficiency. Finally, the DC regulator provides a well regulated  $V_{DC}$  to the constant off-time circuit. The importance of this can be seen by substituting (4) and (5) into (7) and rewriting the expression for  $T_{off}$  as:

$$T_{Off} = \left(\frac{c_{Buf}}{I_{Chg}}\right) \left(\frac{R_3}{R_4}\right) V_{DC} \tag{8}$$

 $T_{Off} = \left(\frac{c_{Buf}}{I_{Chg}}\right) \left(\frac{R_3}{R_4}\right) V_{DC} \tag{8}$  From (8), we see that  $T_{Off}$  is directly proportional to  $V_{DC}$ . Therefore, to ensure low variations in  $T_{off}$ ,  $V_{DC}$  should be well regulated.

## V. MEASURMENT RESULTS AND COMPARISON

### A. Implementation

The proposed system was realized using commercially available discrete components. The load is a sensor node that consists of a MSP430F5594 microcontroller connected to a CC1352R wireless transceiver. Upon power-up, microcontroller is programmed to turn on the CC1352R wireless transceiver, which send a packet every 5 msec until the available energy is consumed. The microcontroller will turn on when  $V_{CAP} = 3.3 \text{ V}$ , and will remain in operation until  $V_{CAP}$  has discharged to 3.0 V. The typical on-time for this sensor node is approximately 30 msec, which includes the boot-up time of the

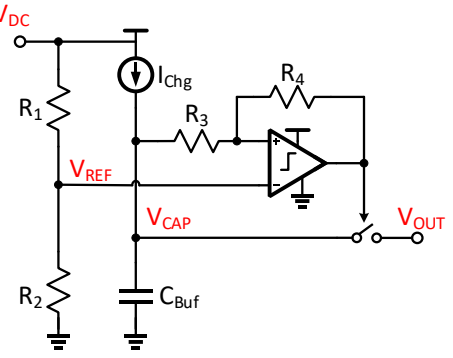


Fig. 5. Schematics for constant charging time circuit.  $V_{out}$  is the final output which is connected to micro controller

microcontroller and the wireless radio and the time for transmission of one or two data packets.

The size of the energy storage capacitor depends on the amount of energy that is required by the sensor node as described by the following equation:

$$C_{Buf} = \frac{2E}{V_{on}^2 - V_{off}^2} \tag{9}$$

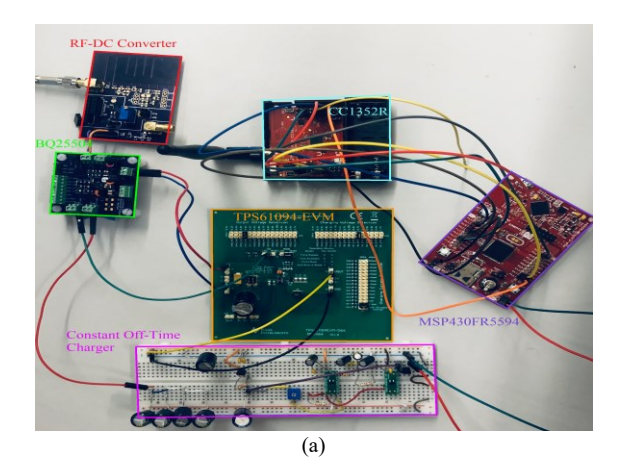
where E is energy in J, and  $V_{on}$  and  $V_{off}$  are the maximum and minimum supply voltages the sensor node requires. It was experimentally determined that the sensor node under consideration requires a minimum of 500 µ J, requiring a minimum capacitance of so 529  $\mu$ F. A final value of  $C_{Buff} = 1$ mF was chosen. The energy storage capacitor is charged using an LM334 from Texas Instruments. The LM334 is an adjustable current source, capable of sourcing a minimum of 10  $\mu$ A, and requires only 1 V of voltage overhead.

The DC regulator was realized using two separate components, the BO25504 battery charger IC [20], and the TPS61094 buck/boost converter, both from Texas Instruments. The BO25504 was chosen for its low startup voltage of 600 mV and its ability to provide the optimum loading of 2.2 k $\Omega$  to the RF-to-DC converter through its maximum point power tracking (MPPT) functionality. One drawback of the BQ25504 is a substantial ripple in the output voltage due to the periodic sampling required for the MPPT. The large ripple is fixed by using the TPS61094 [21] to provide a well-regulated voltage of 4.5 V to the constant off-time circuit. A photograph of the final system is shown in Fig. 6(a).

## VI. MEASURMENT RESULTS AND COMPARISON

With  $C_{Buff} = 1$  mF, and  $I_{Chg} = 10 \mu$ A, an external data logger was used to record the off-time of the sensor node for 80 minutes. An RF signal generator was used to power the system through the RF-to-DC converter directly, and the input power was swept from -4 dBm to +9 dBm in 10-minute increments. For comparison, the same tests were also conducted using two different energy harvester systems: the so-called Baseline system presented in [2], and the P2110 energy harvester from PowerCast Corp. [22]. Both systems were used to power the same MSP430F5594 microcontroller connected to a CC1352R wireless transceiver, as the proposed system.

The measured off-time for all three systems is plotted vs. time in Fig. 6(b). As seen in Fig. 6(b), the measured off-time of the Baseline system and the P2110 both experience extremely large variations in the off-time with increasing RF input power. The proposed system, on the other hand, is relatively stable with



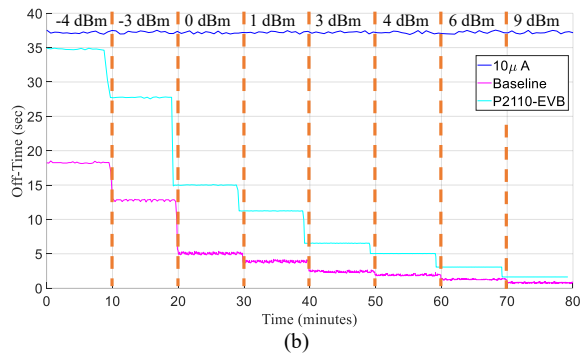


Fig. 6. (a) Test setup for measuring off-time with changes in input RF power, (b) Off-time variation of proposed harvester, baseline harvester, and P2110

an average off-time of approximately 37 sec. It should be mentioned that the minimum RF input power required for operation is -4 dBm for the proposed the proposed system, but is -8 dBm and -10 dBm for the Baseline system and the P2110, respectively.

To quantify the performance of each system over RF input power, we have developed the following figure of merit. We define the mean off-time,  $m_{off}$  in milliseconds, as an array of the mean off-times at each different input power level,  $P_i$ . This is expressed as:

$$m_{Off} = \left[ \mu_{Off(P1)}, \mu_{Off(P2)}, \dots, \mu_{Off(Pi)} \right]$$
 (10)

now, using (9) we define the figure of merit as:

$$FoM = \frac{\max(m_{Off}) - \min(m_{Off})}{\max(P_{RF}) - \min(P_{RF})}$$
(11)

where  $P_{RF}$  is the input RF power expressed in dBm. This FoM was applied to each of the three systems and is shown in Table I. Also shown in Table I are the operating supply voltages, and the minimum RF input power required for operation, referred to as the sensitivity.

The off-time can be reduced in the proposed system by increasing the charging current,  $I_{Chg}$ . To demonstrate this, the above experiment was repeated on the proposed constant off-time circuit for  $I_{Chg} = 10 \,\mu A$ ,  $100 \,\mu A$ , and  $200 \,\mu A$ . For the case of  $I_{Chg} = 200 \,\mu A$ , the off-time is approximately 1.6 sec. This decreased off-time, however, comes at the cost of an increase in the minimum required RF input power. While the

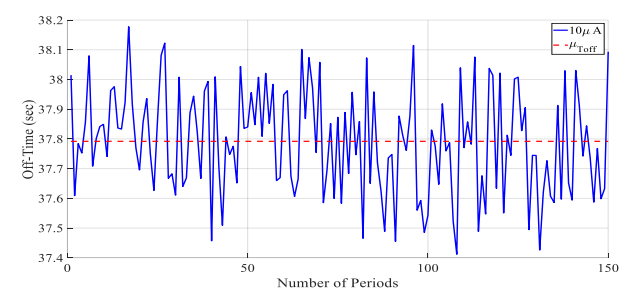


Fig. 7. Measured Off-time using power transmitter

TABLE I: COMPARISON OF SYSTEM PERFORMANCE

	Bassline	P2110	This Work
$V_{DC}$ (V)	3.3	3.3	3.0 to 3.3
Sensitivity (dBm)	-8	-10	-4
FoM	1233	2298	8

TABLE II: BREAKDOWN OF COMPONENT EFFICIENCY

Current	10μΑ	100μΑ	200μΑ
$P_{AVS}(dBm)$	-4	1	4
$\eta_{rect}$	36.6%	55.7%	56.8%
$\eta_{BQ25504}$	40.1%	69.8%	68.8%
$\eta_{TPS61094}$	88.5%	94.1%	93%
$\eta_{overall}$	13.0%	36.6%	36.3%

system operates all the way down to -4 dBm when  $I_{Chg}$  = 10  $\mu A$ , the minimum required RF input power increases to +4 dBm when  $I_{Chg}$  = 200  $\mu A$ . Table II lists the efficiency of each component of the system at different charging rate. It is apparent that the overall system efficiency is dominated by the efficiency of the rectifier, followed by the efficiency of the BQ25504 IC with is performing lower than specification in the datasheet.

Finally, we demonstrate the performance of the proposed system operating in a truly wireless environment. The TX91501b Powercaster transmitter [23] is used for the wireless power transmitter. It operates at 915 MHz with 3 W EIRP, and was placed 2.75 meters away from the sensor node. The sensor node used a simple monopole antenna, tuned for operating at 915 MHz. The charging current was set to  $10~\mu\text{A}$ , and the off-time was measured for 150 complete charge/discharge cycles. The measured off-time is shown in Fig. 7. The mean off-time is 37.8 ms with a standard deviation of 175 ms, or only 0.46%.

# VII. CONCLUSION AND FUTURE WORK

In this paper, we have presented an energy harvester that provides a constant off-time, with very little variation across a wide range of RF input power. Unlike the conventional RF energy harvester, the proposed energy harvester provides precise control of off-time given a minimum threshold input power level. Future work will focus on improving the overall sensitivity of the system and establishing a mechanism to taking advantage of any excess received power.

#### REFERENCES

- [1] M. Satyanarayanan, W. Gao, and B. Lucia, "The computing landscape of the 21st century," in *Proc. 20<sup>th</sup> ACM HotMobile*. New York, NY, USA, Feb. 2019, pp. 45–50. doi: 10.1145/3301293.3302357.
- [2] A. Colin, E. Ruppel, and B. Lucia, "A reconfigurable energy storage Architecture for Energy-harvesting Devices," in *Proc.* 23<sup>rd</sup> ACM

- ASPLOS. New York, NY, USA, Mar. 2018, pp. 767–781. doi: 10.1145/3173162.3173210.
- [3] A. Hoseinghorban, M. R. Bahrami, A. Ejlali, and M. A. Abam, "CHANCE: capacitor charging management scheme in energy harvesting systems," *IEEE Trans. Comput.-Aided Des. Integr. Circuits Syst.*, vol. 40, no. 3, pp. 419–429, Mar. 2021, doi: 10.1109/TCAD.2020.3003295.
- [4] D. Ma, G. Lan, M. Hassan, W. Hu, and S. K. Das, "Sensing, computing, and communications for energy harvesting IoTs: a survey," *IEEE Commun. Surv*, vol. 22, no. 2, pp. 1222–1250, 2020, doi: 10.1109/COMST.2019.2962526.
- [5] S. Kumar, S. De, and D. Mishra, "RF energy transfer channel models for sustainable IoT," *IEEE Internet Things J.*, vol. 5, no. 4, pp. 2817–2828, Aug. 2018, doi: 10.1109/JIOT.2018.2827936.
- [6] V. Deep, V. Narayanan, M. Wymore, D. Qiao, and H. Duwe, "HARC: a heterogeneous array of redundant persistent clocks for batteryless, intermittently-powered systems," in 2020 IEEE RTSS., Huston, TX, Dec. 2020, pp. 270–282. doi: 10.1109/RTSS49844.2020.00033.
- [7] J. Hester et al., "Persistent clocks for batteryless sensing devices," ACM TECS., vol. 15, no. 4, p. 77:1-77:28, Aug. 2016, doi: 10.1145/2903140.
- [8] J. de Winkel, C. Delle Donne, K. S. Yildirim, P. Pawełczak, and J. Hester, "Reliable timekeeping for intermittent computing," in *Proc.* 25<sup>th</sup> ACM ASPLOS. New York, NY, USA: Association for Computing Machinery, Mar. 2020, pp. 53–67. doi: 10.1145/3373376.3378464.
- [9] K. Geissdoerfer and M. Zimmerling, "Learning to communicate effectively between battery-free devices," presented at the 19th USENIX NSDI., Renton, WA, Apr. 2022, pp. 419–435.
- [10] K. Geissdoerfer and M. Zimmerling, "Bootstrapping battery-free wireless networks: efficient neighbor discovery and synchronization in the face of intermittency," presented at the 18th USENIX NSDI, 2021, pp. 439–455.
- [11] U. Muncuk, K. Alemdar, J. D. Sarode, and K. R. Chowdhury, "Multiband ambient RF energy harvesting circuit design for enabling batteryless sensors and IoT," *IEEE Internet Things J.*, vol. 5, no. 4, pp. 2700–2714, Aug. 2018, doi: 10.1109/JIOT.2018.2813162.
- [12] A. Mouapi, N. Hakem, and N. Kandil, "A performance analysis of schottky diode to support RF energy harvesting," in 2019 IEEE Int. Symp. on Antennas and Propagation and USNC-URSI Radio Science Meeting, Jul. 2019, pp. 1169–1170. doi: 10.1109/APUSNCURSINRSM.2019.8888832.

- [13] A. Mouapi, N. Hakem, and N. Kandil, "Analysis of schottky multistage voltage doubler rectifiers for RF energy harvesting applications," in 2020 IEEE Int. Symp. on Antennas and Propagation and North American Radio Science Meeting, Jul. 2020, pp. 1327–1328. doi: 10.1109/IEEECONF35879.2020.9330084.
- [14] S. Muhammad, J. J. Tiang, S. K. Wong, A. Smida, R. Ghayoula, and A. Iqbal, "A dual-band ambient energy harvesting rectenna design for wireless power communications," *IEEE Access*, vol. 9, pp. 99944–99953, 2021, doi: 10.1109/ACCESS.2021.3096834.
- [15] G. Verma and V. Sharma, "A novel RF energy harvester for event-based environmental monitoring in wireless sensor networks," *IEEE Internet Things J.*, vol. 9, no. 5, pp. 3189–3203, Mar. 2022, doi: 10.1109/JIOT.2021.3097629.
- [16] S. Kim et al., "Ambient RF energy-harvesting technologies for self-sustainable standalone wireless sensor platforms," in *Proc. IEEE*, vol. 102, no. 11, pp. 1649–1666, Nov. 2014, doi: 10.1109/JPROC.2014.2357031.
- [17] V. Deep et al., "Experimental study of lifecycle management protocols for batteryless intermittent communication," in 18th IEEE MASS, Oct. 2021, pp. 355–363. doi: 10.1109/MASS52906.2021.00052.
- [18] "10.14: Friis Transmission Equation," Engineering LibreTexts, Apr. 02,2020. https://eng.libretexts.org/Bookshelves/Electrical\_Engineering/Electro-Optics/Book%3A\_Electromagnetics\_II\_(Ellingson)/10%3A\_Antennas/1 0.14%3A Friis Transmission Equation
- [19] J. F. Dickson, "On-chip high-voltage generation in MNOS integrated circuits using an improved voltage multiplier technique," *IEEE J. Solid-*State Circuits, vol. 11, no. 3, pp. 374–378, Jun. 1976, doi: 10.1109/JSSC.1976.1050739.
- [20] "BQ25504 data sheet, product information and support | Tl.com." https://www.ti.com/product/BQ25504?dcmp=dsproject&hqs=pf
- [21] "TPS61094 data sheet, product information and support | TI.com." https://www.ti.com/product/TPS61094
- [22] A. Khalifeh, M. Saadeh, K. A. Darabkh, and P. Nagaradjane, "Radio-frequency based energy charging- an experimental study," in 2nd IEEE MENACOMM., Bahrain, Nov. 2019, pp. 1–4. doi: 10.1109/MENACOMM46666.2019.8988585.
- [23] "Powercaster Transmitter," Powercast Co. https://www.powercastco.com/products/powercaster-transmitter